Zajcsuk, L. and Habib, G. and Zelei, A.: Antropomorfic parameters of a nonlinear dynamic model of self sustained hopping. DSTA 2019, Dec 2-5, 2019, Lodz, POLAND.

Antropomorfic parameters of a nonlinear dynamic model of self sustained hopping

Liliána Zajcsuk, Giuseppe Habib, Ambrus Zelei

Abstract: In this work, we study the dynamics of legged locomotion adopting a combination of experiments and mathematical models. Our recently developed planar model is capable of self-sustained human-like hopping motion. However, the biomechanical indicators, such as joint angle ranges, joint velocities and joint torques which provide stable motions are not compatible with realistic parameter values. In general, parameters can be optimized with respect to a variety of cost functions, such as energy efficiency, impact reduction, locomotion speed or hopping height. In contrast to these performance measures, our current objective is to minimize the gap between the measurement and simulation results of human locomotion in terms of the aforementioned biomechanical indicators. This will finally provide realistic anthropomorphic motion, reducing the gap between real life legged locomotion and locomotion based on mathematical models.

1. Introduction

The dynamic analysis of legged locomotion via mathematical models is common in the literature [2, 10]. One of the most simple models is the spring loaded inverted pendulum (SLIP) model of running [3, 10, 11]. Some other models were developed which catch the geometry of the human leg more precisely, e.g., the segmented leg model in [20] provides stable locomotion. Although, our ultimate goal is the analysis of the biomechanics of running (we started in [26]), we believe that the dynamic analysis of hopping locomotion is a proper preliminary study. The dynamic model of a hopping locomotor is less complex than running motion, because only one leg (or two legs moving together) is modeled. We developed a self-stable model of human hopping locomotion and published the main properties in [28].

Prior to the model extension, our goal is to tune physical parameters in order to reach human-like and feasible motion both in terms of kinematic and dynamic characteristics. This is achieved by tuning the control parameters with which the simulated motion is as close as possible to the experimentally obtained motion. In the present paper, we collect the experimental data from the literature and introduce the cost function that we use for the parameter optimization.

Having a well-tuned (human-like) model, we will be able to perform the sensitivity analysis of the parameters and to discover the optimality principles (similarly as in [5]) in future studies. This is especially advantageous, when biomechanical experiments cannot clearly uncover the parameter effects. For instance we will be able to analyse the effect of the foot strike pattern on the impulsive ground reaction forces and energetic costs. Although, there are uncertainties in the experimental studies, as it is mentioned in [1].

To cite: [**?**].

2. The hopping model

The sagittal plane model of human hopping locomotion consists of the equations of motion of the multibody system shown in Fig. 1. Besides, a controller is an inseparable part of the mathematical model. The model published in [6] was further developed in [27, 28, 25]:

- The strike index (see s in Fig. 1) can be varied.
- The locomotion can be analysed on uphill or downhill terrain too (see ψ in Fig. 1).
- It is checked, whether the ground-foot friction force exceed the limiting value.
- A multi-level (partial) feedback controller guarantees that the desired locomotion speed and the desired hopping elevation is accurately maintained regardless the possible perturbations coming from the environment.

The main characteristics of the model are:

- It contains similar geometric nonlinearities as the human body, i.e., the geometry is not oversimplified such as in case of the SLIP model.
- The impulsive forces at the initial ground-foot contact are considered in the model and therefore the impact induced kinetic energy loss (constrained motion space kinetic energy CMSKE [14, 12, 13]) is taken into account.
- An active controller maintains the energy level and the stable periodic motion.
- The model and the calculations are formulated in such way that they can be easily applied for more complex multibody models of locomotion.

2.1. Mechanical part of the model

As Fig. 1 shows, the mechanical model consist of the foot, the shank and the thigh (masses m_i and lengths l_i; $i = 1 \dots 3$ respectively). Rotational springs with stiffness k_{B} and k_{C} maintain the joint angles. Furthermore, a reaction wheel (with mass m_{r} and mas moment of inertia J_{r}), which is connected in the hip, prevents fallover. One period of locomotion consists of the flight (airborne) phase and the ground (stance) phase. These continuous phases are separated by the events respectively, when the point A reaches the ground, and when the ground-foot contanct force becomes zero. For more details and model assumptions (frictionless joints, no rebound or slip of the foot, smooth terrain), see [6, 28, 25].

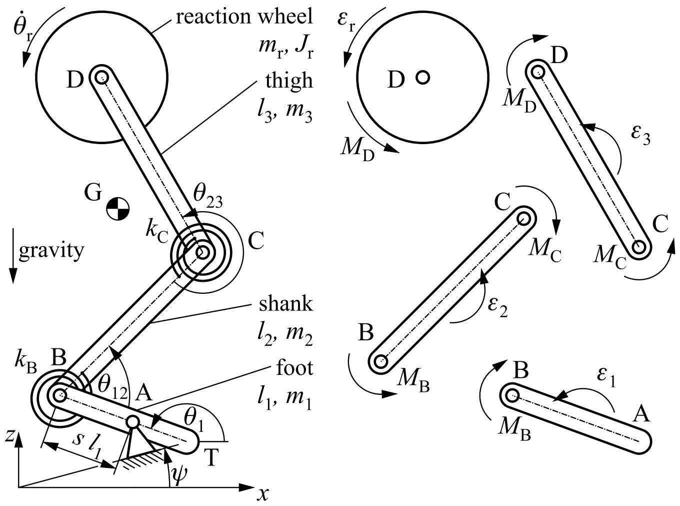

Figure 1. A simplified segmental multibody model of the human body in the sagittal plane.

2.2. Control part of the model

Separate control law is defined for the ground phase and the flight phase (see (1) and (2) repectively):

$$\begin{bmatrix} M_B^F \\ M_C^F \\ M_D^F \end{bmatrix} = \begin{bmatrix} -D_B\dot{\theta}_{12} \\ -D_C\dot{\theta}_{23} \\ P(x_A - (x_G + x_\Delta)) + D(\dot{x}_A - \dot{x}_G) \end{bmatrix} \quad (1)$$

$$\begin{bmatrix} M_B^G \\ M_C^G \\ M_D^G \end{bmatrix} = \begin{bmatrix} P_E(E - E_0)\,\mathrm{sgn}(\dot{\theta}_{12}) \\ P_E(E - E_0)\,\mathrm{sgn}(-\dot{\theta}_{23}) \\ -P_r\theta_r - D_r\dot{\theta}_r \end{bmatrix} \quad (2)$$

Flight phase: The vibrations are supressed by torques M_B^F and M_C^F. The tiptoe position x_A is stabilized about the nominal horizontal position $x_G + x_\Delta$ by the proportional-derivative (PD) controller realized by M_D^F. Parameters D_B, D_C, P and D in (1) are control gains. In the foot landing preparation, zero moment pole (ZMP) control [10, 24], is achieved by $x_\Delta = P_\Pi\,\Pi_A - K_v$, where Π_A is the angular momentum about the point A, P_Π is a control gain and K_v is a control parameter that affects the locomotion speed.

Ground phase: The overall mechanical energy is stabilized around the target energy level E_0 by means of the control torques M_B^G and M_C^G. To prevent the continuous growth of the angular velocity $\dot{\theta}_r$, the torque M_D^G stabilizes the position of the reaction wheel. Variables P_E, P_r and D_r are control gains.

2.3. Parameters to tune

The control law defined in (1) and (2) guarantees hopping-like periodic motion in a certain range of the parameters [28]. The goal of the present study is to tune the parameters in such way that the hopping motion is not only stable, but the achieved motion characteristics are human-like and realistic, i.e., the cost function in Section 4 is minimal. The variable control parameters are: D_{B}, D_{C}, P, D, P_{Π}, K_v, P_E, P_{r}, D_{r}, E_0. Some physical parameters can be also tuned: the spring stiffnesses k_{B} and k_{C} and the ankle and knee joint angles α_{12} and α_{23} which belongs to the unstretched springs. The goal in Section 4 is to find the point in this $p = 14$ dimensional parameter space $\mathbf{p} = [D_{\mathrm{B}}, D_{\mathrm{C}}, P, D, P_{\Pi}, K_v, P_E, P_{\mathrm{r}}, D_{\mathrm{r}}, E_0, k_{\mathrm{B}}, k_{\mathrm{C}}, \alpha_{12}, \alpha_{23}]$, where the motion characteristics are the closest to the curves which are presented in Section 3.

3. Collection of biomechanical data from the literature

In order to tune the hopping model (presented in Fig. 1) in such way that the simulated time history of the joint angles, the joint torques and the joint powers are realistic and feasible, we have acquired measurement data from the literature. Because of the controversies found, we analysed the data statistically.

Measurement data from articles by Ahn et al [1], Caekenberghe et al [23], Goss [8], Liu [15], Mann [16], and Novacheck [18] were used. The original datasets are not available, therefore they have to be extracted from the presented graphs in articles. After setting the origo and the scales of the axes, 20 points on each graph were pointed manually. It is important to note, that the obtained datasets have small errors compared to the original measurement data, because the points were chosen manually, and the resolution of the screen and the accuracy of the human eye and the mouse have limitations. Spline-interpolation was applied on the sets of 20 points and the average and variance were calculated for each set.

Due to lack of measurement data about the full running cycle, only the stance phase was concerned. Therefore, the initial contact was considered to $t_0 = 0\%$, and the end, the "toe off" was set to $t_{\mathrm{e}} = 100\%$. The proportion of the stance phase during running varies strongly, depending on personal attributes. According to [18], it is generally below 50%, and its minimal length can be 22% of the running cycle for the best sprinters. In our case, its length was set to 40%, estimating an average value.

The results can be seen in the Fig. 2-10. The black thick line without markers represents the average and the grey area shows the variance. The differences of the obtained data from the different resousces can be caused by several factors, including individual ones, e.g., age [17], sex [22], and ethnicity-race [21] can cause differences in the anatomy, which affect the gait [19, 7, 4]. Some of the runners were professional and trained, specialized in long-term running or short-term sprinting, while other subjects were not necessarily expe-

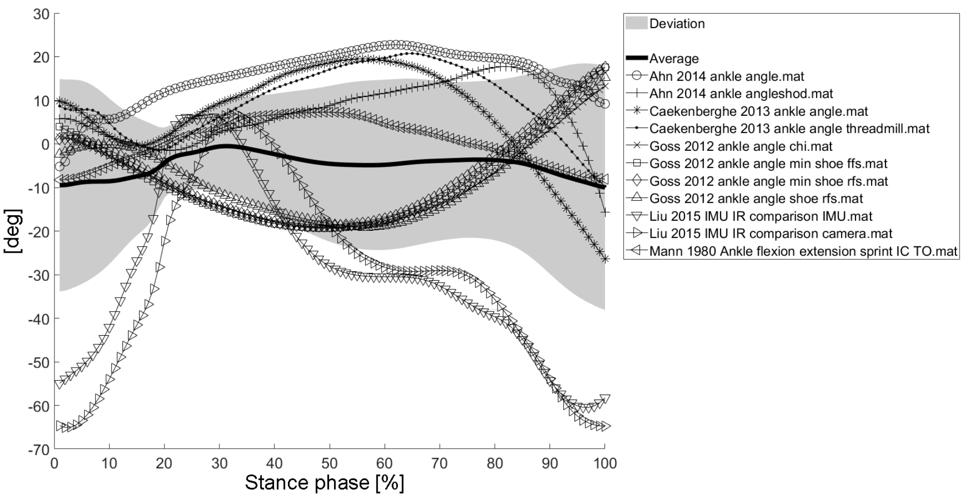

Figure 2. Ankle angle during the stance phase

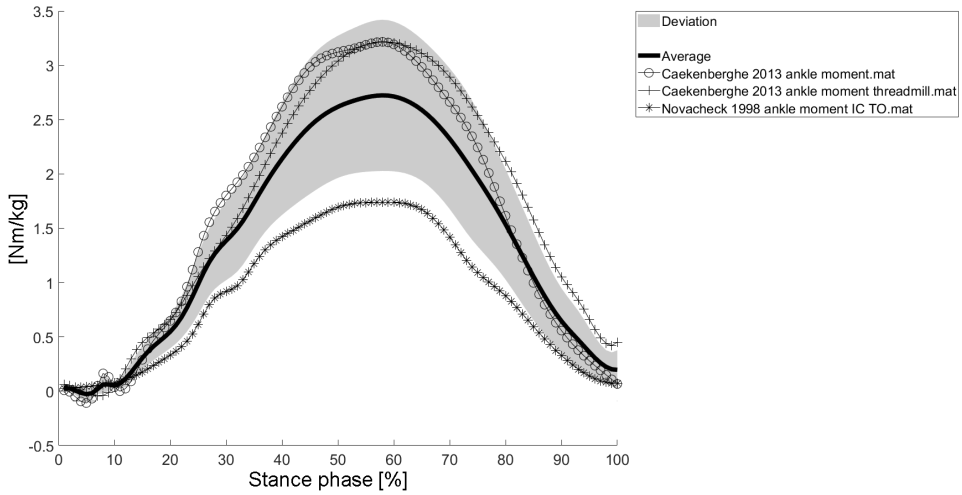

Figure 3. Ankle torque during the stance phase

rienced athletes; however, the participants were healthy, without any injury related to the musculoskeletal or nervous system. The used measurement devices and the environmental conditions were also different. The participants were running at different speed for each measurement which causes changes in the kinematics, and the stiffness of the surface may also influence the running strategy [9]. Some measurements were taken on treadmill. Still, these data can be applied for model tuning. We collected the ankle angle α_a, the ankle torque τ_a, the ankle power P_a, the knee angle α_k, the knee torque τ_k, the knee power P_k,

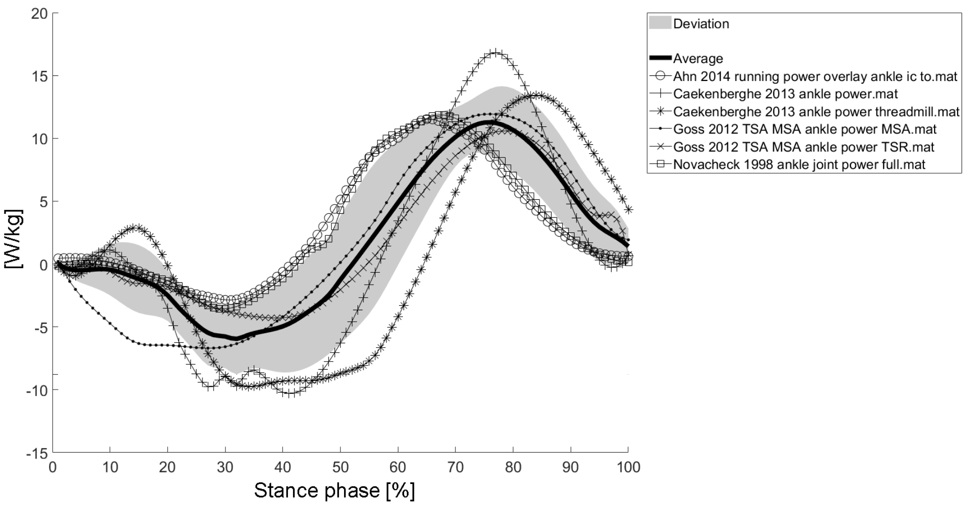

Figure 4. Ankle power during the stance phase

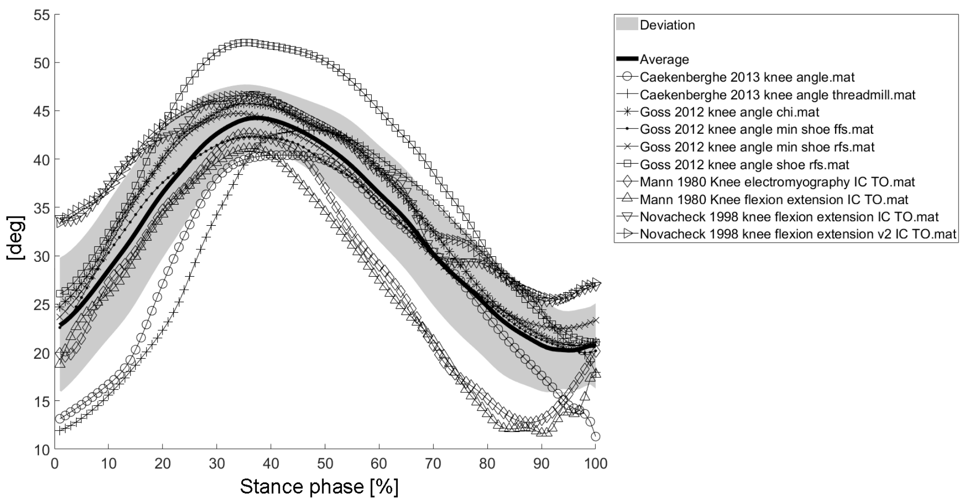

Figure 5. Knee angle during the stance phase

the hip angle α_h, the hip torque τ_h and the hip power P_h, as it is detailed below.

- Ankle angle (shown in Fig 2): For this quantity, relatively large difference was expected among the different resources, because the different running strategies (forefoot and rearfoot strike) highly influence the ankle angle. As it can be seen, the average of the ankle angle values is not the best way to approximate a real movement, because it stays between -10 and 0 degrees. The datasets from each measurement have fair

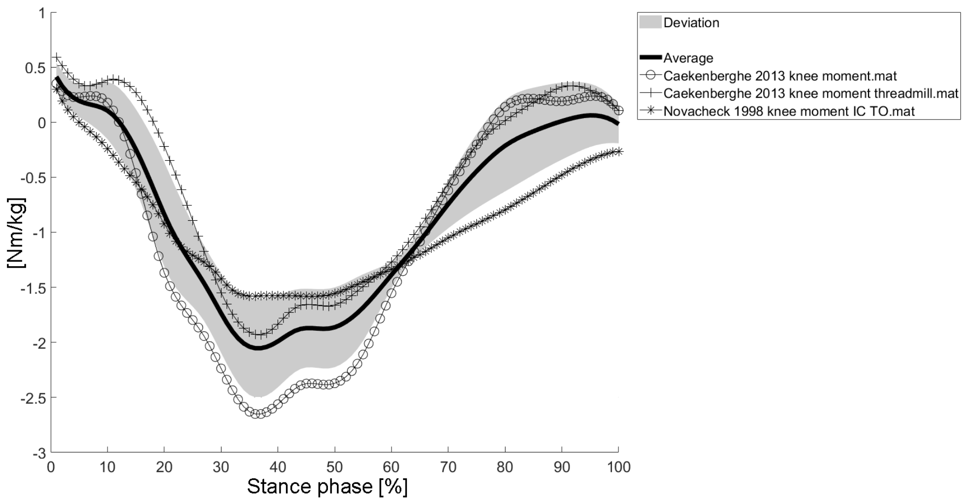

Figure 6. Knee torque during the stance phase

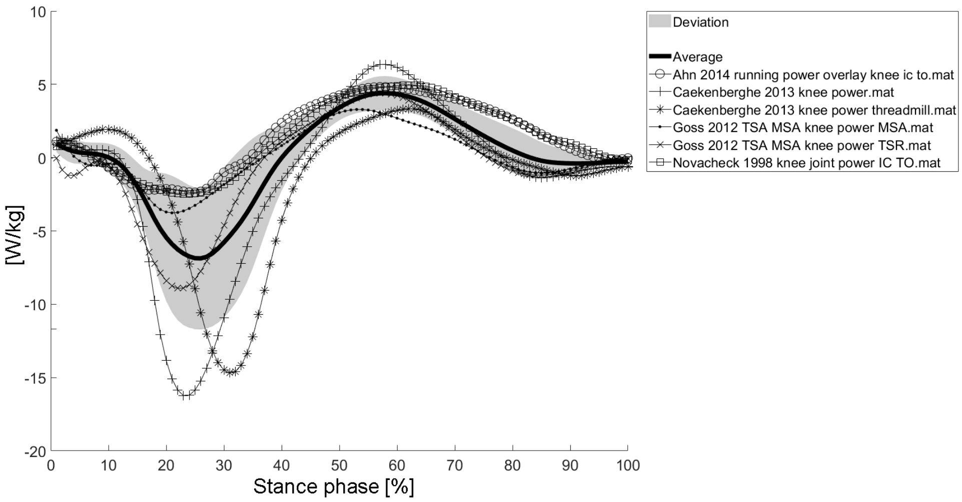

Figure 7. Knee power during the stance phase

difference, the variance is high compared to other datasets' variances.

- Ankle torque (shown in Fig 3): The obtained graphs have similar characteristics and relatively small variance, therefore using the average as estimation of the human running is fair. The graphs show that the maximum magnitude ankle torque is exerted in the mindle of the stance phase.
- Ankle power (shown in Fig 4): The obtained graphs have similar characteristics and

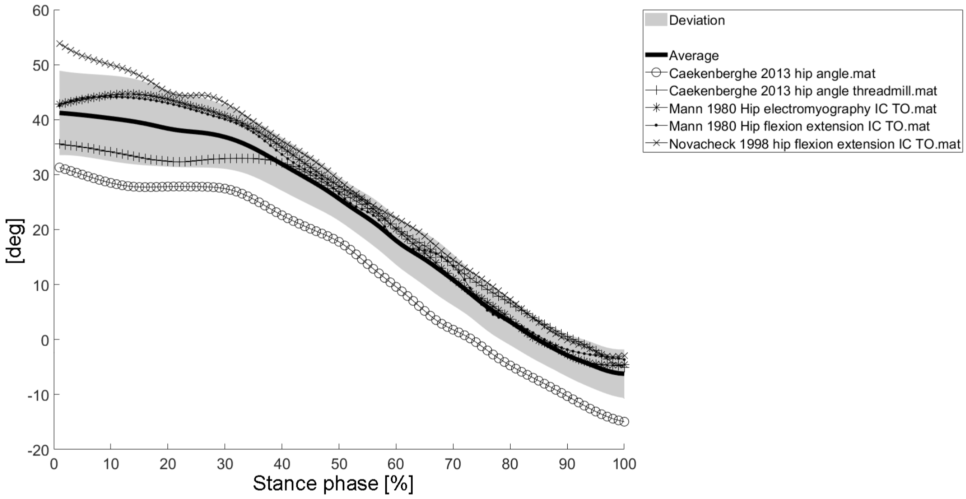

Figure 8. Hip angle during the stance phase

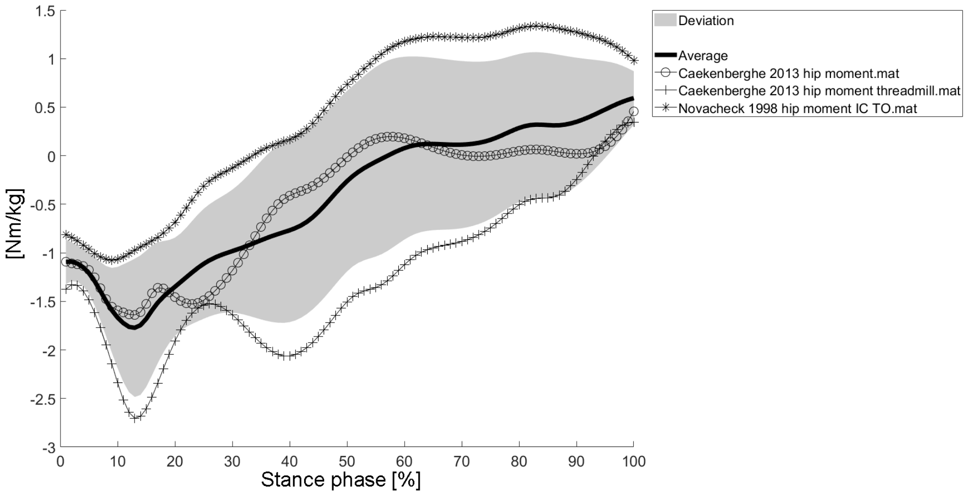

Figure 9. Hip torque during the stance phase

relatively small variance compared to other datasets, therefore using the average as estimation of the human running is fair. The graphs show that negative power (absorption of mechanical energy) is realized in the first half of the stance phase. Positive power (acceleration of the segments) is observable in the second half of the stance phase. Note that the positive peak is three times higher than the negative peak. It refers to the fact that the ankle torque contributes in the propulsion of the body

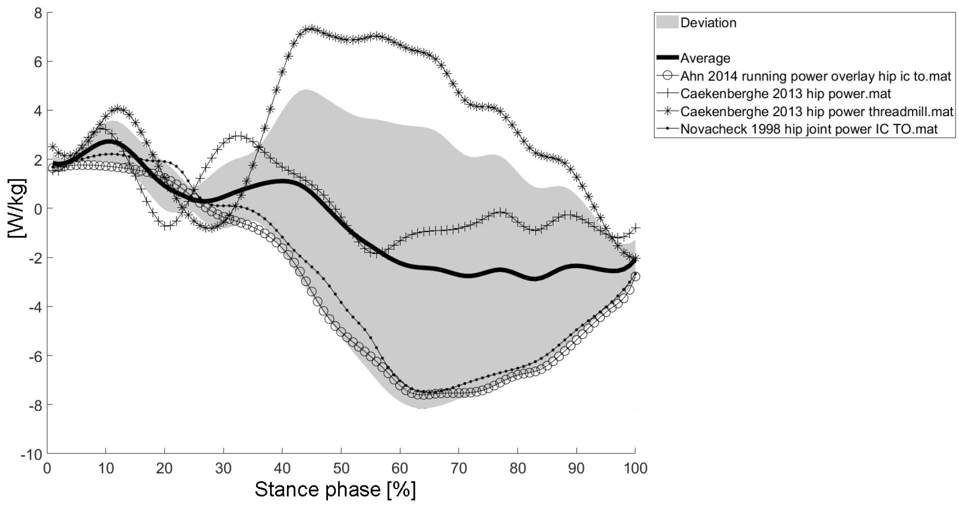

Figure 10. Hip power during the stance phase

rather than in the damping of the ground-foot collision.

- Knee angle (shown in Fig 5): For this quantity, a quite large amount of data was available. They all have similar characteristics, therefore the average can be considered as a good estimation.
- Knee torque (shown in Fig 6): The obtained graphs have similar characteristics and relatively small variance, therefore using the average as estimation of the human running is fair. The shape of the knee torque is in correlation with the ankle torque: the maximum is in the middle.
- Knee power (shown in Fig 7): The variance of the data is fair. The negative peak in the first part of the stance phase is much larger than the positive peak in the second half of the stance phase. We can drive the conclusion that knee contributes more in the energy absorbtion at the ground-foot collision than in the propulsion of the body. This is the opposite compared to the ankle behaviour.
- Hip angle (shown in Fig 8): The obtained graphs have similar characteristics and relatively small variance, therefore using the average as estimation of the human running is fair.
- Hip torque (shown in Fig 9): Only three datasets were available, and two of them are from the same paper. All have similar, ascending characteristics. For future investigations, acquiring more data could improve the quality.
- Hip power (shown in Fig 10): According to the literature, running on a treadmill does not cause any difference in the kinetic parameters. However, the power of the

hip definitely changes. The cause of this phenomena should be investigated in the future.

Despite of the several possibilities to improve the data set, the current method and acquired data can be considered suitable for tuning the mechanical model.

4. Cost function and parameter tuning

Our goal is to tune the parameters $\mathbf{p} \in \mathbb{R}^{14}$ in such way that the scalar cost function $F(\mathbf{p})$, which is composed by the experimental data shown in Section 3 and the simulated data, is minimal. The cost function is formulated by using the experimental data collected in a vector: $\mathbf{V}(t) = [\alpha_\mathrm{a}(t), \tau_\mathrm{a}(t), P_\mathrm{a}(t), \alpha_\mathrm{k}(t), \tau_\mathrm{k}(t), P_\mathrm{k}(t), \alpha_\mathrm{h}(t), \tau_\mathrm{h}(t), P_\mathrm{h}(t)]^\mathrm{T}$:

$$F(\mathbf{p}) = \int_0^{t_\mathrm{e}} \Big(\mathbf{V}(t) - \tilde{\mathbf{V}}(\mathbf{p}, t)\Big)^\mathrm{T} \mathbf{W} \Big(\mathbf{V}(t) - \tilde{\mathbf{V}}(\mathbf{p}, t)\Big) \,\mathrm{d}t, \tag{3}$$

where the time histories coming from the simulated motion with parameter set $\mathbf{p}$ are collected in $\tilde{\mathbf{V}}(\mathbf{p}, t) = [\tilde{\alpha}_\mathrm{a}(\mathbf{p}, t), \tilde{\tau}_\mathrm{a}(\mathbf{p}, t), \tilde{P}_\mathrm{a}(\mathbf{p}, t), \tilde{\alpha}_\mathrm{k}(\mathbf{p}, t), \tilde{\tau}_\mathrm{k}(\mathbf{p}, t), \tilde{P}_\mathrm{k}(\mathbf{p}, t), \tilde{\alpha}_\mathrm{h}(\mathbf{p}, t), \tilde{\tau}_\mathrm{h}(\mathbf{p}, t), \tilde{P}_\mathrm{h}(\mathbf{p}, t)]^\mathrm{T}$, and the weight matrix $\mathbf{W} \in \mathbb{R}^{9\times 9}$ is diagonal with $W = \mathrm{diag}(w_1, \ldots, w_9)$. For first trial, $\mathbf{W}$ is chosen as identity.

For demonstration purposes, we show a simulation result in the human-like range of locomotion speed (0.15 m/s) and hopping elevation (10 cm). Here, the parameters in $\mathbf{p}$ are adopted from [28]. Fig. 11 shows the stroboscopic view of the hopping motion on flat surface. The corresponding cost functions are collected in Fig. 12. These are compared with the experimental results shown in Section 3.

In case of the joint angles (upper three panels), the simulation results are fair. Even the experimentally obtained ankle angles have controversies, thus we couldn't expect good correspondence of the measurements and the simulations. The simulated knee angle time history is quite close to the experiments. The trends of the hip angle curve are also good, however it could be enhanced quantitatively.

The joint torques in the middle row of Fig. 12 seem unnatural comparing to the experimental data. It is caused by the ground-to-flight and flight-to-ground switches of the controller and by the artifically introduced saturation of the torques. Consequently, not only the parameter tuning but the review of the control law equations (1) and (2). The abrupt switching should be avoided.

The most important difference of the mechanical power of the joint torques from the experimental data is that the controller intentionally ensures positive power in the entire ground phase. This induces again the review of the control law. However, the magnitude of the mechanical power is realistic.

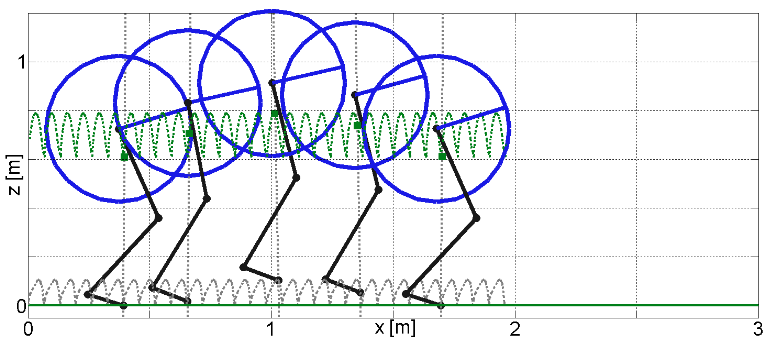

Figure 11. Stroboscopic view of the hopping motion

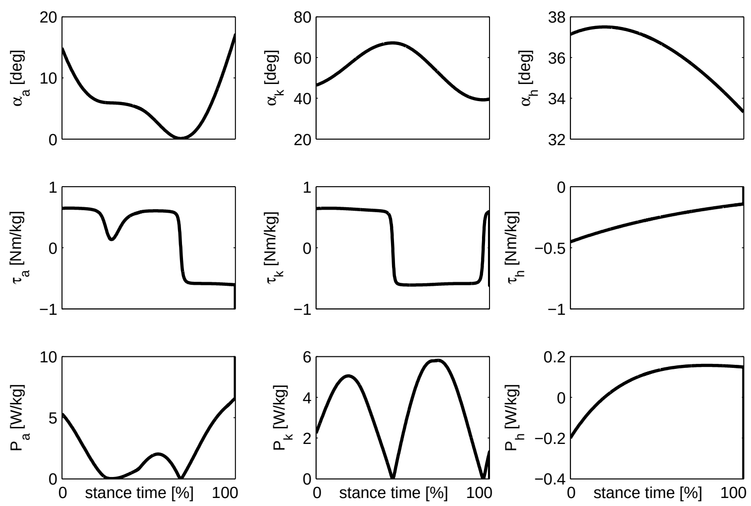

Figure 12. Components of the cost funcion in case of a typical simulation result: $\alpha_{\mathrm{a}}(t)$, $\tau_{\mathrm{a}}(t)$, $P_{\mathrm{a}}(t)$, $\alpha_{\mathrm{k}}(t)$, $\tau_{\mathrm{k}}(t)$, $P_{\mathrm{k}}(t)$, $\alpha_{\mathrm{h}}(t)$, $\tau_{\mathrm{h}}(t)$, $P_{\mathrm{h}}(t)$.

5. Conclusions

We have collected experimental data from the literature for the joint angles, joint torques and the joint power for human running. We have shown that most of these data can be used as a template motion pattern, and we formulated a cost function with which the model parameters are tuned. The experimental data were compared to the not yet optimized simulated motion and we have concluded that in spite of the fact that the joint angles are fair, the joint torques and power are not realistic because of the nature of the controller. The parameter optimization will be done (in future work) after the review of the control law.

For future investigations, there are several ways to improve the data collection. Using larger amount of input data can lead to more supported result, which is much closer to the "average" human running. The data collection from graphs can be fully automatized. Creating new measurement data, the same conditions and methods can surely be applied for each individual, e.g., the movement of all participants is recorded with the same equipment, the data is evaluated with the same method, and the participants runs with the same speed. In future work, the measurement dataset will be categorized based on age, sex and training level. For these different datasets, different model parameters will be found.

Acknowledgments

This work was supported by the The Higher Education Excellence Program of the Ministry of Human Capacities in the frame of Biotechnology research area of Budapest University of Technology and Economics (BME FIKP-BIO), by the Hungarian National Research, Development and Innovation Ofce (Project id.: NKFI-FK18 128636), by the National Research, Development and Innovation Fund (TUDFO/51757/2019-ITM, Thematic Excellence Program) and by the Hungarian-Chinese Bilateral Scientific and Technological cooperation Fund under Grant No. 2018-2.1.14-TET-CN-2018-00008.

References

[1] Ahn, A., Brayton, C., Bhatia, T., and Martin, P. Muscle activity and kinematics of forefoot and rearfoot strike runners. *Journal of Sports and Health Science 3*, 1 (2014), 102–112. doi:10.1016/S0966-6362(97)00038-6.

[2] Alexander, R. M. Simple models of human movement. *Applied Mechanics Reviews 48*, 4 (1995).

[3] Blickhan, R., and Full, R. J. Similarity in multilegged locomotion: Bouncing like a monopode. *Journal of Comparative Physiology A: Neuroethology, Sensory, Neural Behavioral Physiology 173*, 5 (1993), 509–517. doi:10.1007/BF00197760.

[4] Chumanov, E. S., Wall-Scheffler, C., and Heiderscheit, B. C. Gender differences in walking and running on level and inclined surfaces. *Clinical Biomechanics 23*, 10 (2008), 1260–1268. doi:/10.1016/j.clinbiomech.2008.07.011.

[5] Clever, D., Hu, Y., and Mombaur, K. Humanoid gait generation in complex environments based on template models and optimality principles learned from human beings. *Intl. Journal of Robotics Research* (2018), 21 pages. doi.org/10.1177/0278364918765620.

[6] Fekete, L., Krauskopf, B., and Zelei, A. Three-segmented hopping leg for the analysis of human running locomotion. In *The 9th European Nonlinear Dynamics Conference (ENOC 2017)* (Budapest, Hungary, June, 25 – 30 2017), pp. 1–2.

[7] Ferber, R., McClay Davis, I., and Williams III, D. S. Gender differences in lower extremity mechanics during running. *Clinical Biomechanics 18*, 4 (2003), 350–357. doi:/10.1016/S0268-0033(03)00025-1.

[8] Goss, D. L. *A Comparison of Lower Extremity Joint Work and Initial Loading Rates among Four Different Running Styles*. PhD thesis, University of North Carolina at Chapel Hill, 2012.

[9] Hardin, E. C., van den Bogert, A. J., and Hamill, J. Kinematic adaptations during running: Effects of footwear, surface, and duration. *Medicine & Science in Sports & Exercise*.

[10] Holmes, P., Full, R. J., Koditschek, D. E., and Guckenheimer, J. The dynamics of legged locomotion: Models, analyses, and challenges. *SIAM Rev. 48*, 2 (2006), 207–304.

[11] Hutter, M., Remy, C. D., Hopflinger, M. A., and Siegwart, R. Slip running with an articulated robotic leg. In *The 2010 IEEE/RSJ International Conference on Intelligent Robots and Systems* (Taipei, Taiwan, 18-22 October 2010), pp. 4934–4939.

[12] Jungers, W. L. Barefoot running strikes back. *Nature, Biomechanics 463*, 7280 (2010), 433–434.

[13] Kövecses, J., and Kovács, L. L. Foot impact in different modes of running: mechanisms and energy transfer. *Procedia IUTAM 2* (Symposium on Human Body Dynamics, 2011), 101–108.

[14] Lieberman, D. E., Venkadesan, M., Werbel, W. A., Daoud, A. I., D'Andrea, S., Davis, I. S., Mang'Eni, R. O., and Pitsiladis, Y. Foot strike patterns and collision forces in habitually barefoot versus shod runners. *Nature, Biomechanics 463*, 7280 (2010), 531–535. doi:10.1038/nature08723.

[15] Liu, S. T.-T. A wearable gait analysis system for overstriding in runners, 2015. Bachelor's thesis, Harvard College.

[16] Mann, R. A., and Hagy, J. Biomechanics of walking, running and sprinting. *The American Jornal of Sports Medicine 8*, 5 (1980), 345–350.

[17] Narici, M. V., Maganaris, C. N., Reeves, N. D., and Capodaglio, P. Effect of aging on human muscle architecture. *Journal of Applied Physiology 95*, 6 (2003), 2229–2234. doi:/doi.org/10.1152/japplphysiol.00433.2003.

[18] Novacheck, T. F. The biomechanics of running. *Gait and Posture 7*, 1 (1998), 77–95. doi:/10.1016/S0966-6362(97)00038-6.

[19] Phinyomark, A., Hettinga, B. A., Osis, S. T., and Ferber, R. Gender and age-related differences in bilateral lower extremity mechanics during treadmill running. *PLoS ONE 9*, 8 (2014), e105246. doi:/10.1371/journal.pone.0105246.

[20] Rummel, J., and Seyfarth, A. Stable running with segmented legs. *Intl. Journal of Robotics Research 27*, 8 (2008), 919–934.

[21] Santos-Concejero, J., Granados, C., Irazusta, J., Bidaurrazaga-Letona, I., Zabala-Lili, J., Tam, N., and Gil, S. Differences in ground contact time explain the less efficient running economy in north african runners. *Biology of Sport 30*, 3 (2013), 181–187. doi:/doi.org/10.5604/20831862.1059170.

[22] Shultz, S. J., Nguyen, A.-D., and Schmitz, R. J. Differences in lower extremity anatomical and postural characteristics in males and females between maturation groups. *Journal of Orthopaedic & Sports Physical Therapy 38*, 3 (2008), 137149. doi:/doi.org/10.2519/jospt.2008.2645.

[23] Van Caekenberghe, I., Segers, V., Aerts, P., Willems, P., and De Clercq, D. Joint kinematics and kinetics of overground accelerated running versus running on an accelerated treadmill. *Journal of the Royal Society Interface 10*, 84 (2013), 77–95. doi:10.1098/rsif.2013.0222.

[24] Westervelt, E. R., Grizzle, J. W., Chevallereau, C., and et al. *Feedback Control of Dynamic Bipedal Robot Locomotion*. CRC Press, 2007.

[25] Zelei, A., Bencsik, L., Insperger, T., and Stpn, G. Stable internal dynamics of a legged hopping model with locomotion speed control. In *15th IFToMM World Congress* (Krakow, Poland, 30, June - 4 July 2019), p. 10 pages.

[26] Zelei, A., Bencsik, L., Kovács, L. L., and Stépán, G. Energy efficient walking and running - impact dynamics based on varying geometric constraints. In *12th Conference on Dynamical Systems Theory and Applications* (Lodz, Poland, 2-5, December 2013), pp. 259–270.

[27] Zelei, A., and Insperger, T. Reduction of ground-foot impact intensity of a hopping leg model on slopes. In *5th Joint International Conference on Multibody System Dynamics - IMSD 2018* (Lisbon, Portugal, 24-28, June 2018), p. 2 pages extended abstract.

[28] Zelei, A., Krauskopf, B., Piiroinen, P. T., and Insperger, T. Stable periodic motion of a controlled segmented leg model of pedal locomotion with inelastic ground-foot collision. *Nonlinear Dynamics 97*, 3 (2019), 1945–1958. doi:10.1007/s11071-019-04911-z.

Liliána Zajcsuk, B.Sc.: Budapest University of Technology and Economics, Muegyetem rkp. 3. Budapest, H-1111, Hungary (*lilizajcsuk@gmail.com*).

Giuseppe Habib, Ph.D.: MTA-BME Lendület Human Balancing Research Group, Muegyetem rkp. 3. Budapest, H-1111, Hungary (*habib@mm.bme.hu*).

Ambrus Zelei, Ph.D.: MTA-BME Research Group on Dynamics of Machines and Vehicles, Muegyetem rkp. 3. Budapest, H-1111, Hungary (*zelei@mm.bme.hu*).